Available online at www.sciencedirect.com

ScienceDirect

Procedia Structural Integrity 38 (2022) 447–456

Structural Integrity Procedia

www.elsevier.com/locate/procedia

Fatigue Design 2021, 9th Edition of the International Conference on Fatigue Design

Residual stresses influence on the fatigue strength of structural components

A. Chiocca[a,*], F. Frendo[a], L. Bertini[a]

[a]*Department of Civil and Industrial Engineering, University of Pisa, Largo Lucio Lazzarino 2, Pisa 56122, Italy*

Abstract

Several production processes, both conventional and innovative, may result in residual stresses arising in critical areas of a component. The main issues include high distortion, reduced fatigue life, fracturing or delamination. In this context, standard fatigue design codes traditionally consider residual stresses through conservative assumptions, leading to either sub-optimal design or unexpected failures. Recently, innovative computational techniques have been developed to address residual stresses in a more comprehensive way. As a result, a more effective material utilisation and a more accurate fatigue life assessment can be achieved. The present work examines the influence of residual stresses on the fatigue endurance of S355JR structural steel components. Both welded and notched components were analysed, carrying out numerical and experimental analyses. In the case of welded components, residual stresses resulting from the welding process were numerically evaluated by means of an uncoupled thermal-structural simulation, while for notched specimens a preload causing limited yielding was used to induce a local residual stress field comparable to that obtained for welded specimens nearby the critical locations. Even if he work is still in progress, tests carried out with different specimens under different loading conditions allowed to understand the effect of residual stresses on the fatigue life.

Keywords: residual stresses; fatigue; thermal-structural simulation; welding; S355JR

1. Introduction

Welding is one of the most common manufacturing processes used to join metal components togheter and is of great importance because of all the advantages this process offers. These include design flexibility, ease of use in the automated production process, weight and cost savings. Unfortunately, there are also disadvantages that may preclude its application in some areas. The most common problems include misalignment [19], ease of fracture [12], reduction of the buckling resistance [28], reduction of fatigue life [2] and generation of high residual tensile stresses [18]. The most common issues are caused by the highly non-linear localised heat generated in a defined volume leading to expansions and contractions of the material and causing high plastic deformations. For these reasons, particular atten-

* Corresponding author. Tel.: +39-050-2218011 ;
E-mail address: andrea.chiocca@phd.unipi.it

10.1016/j.prostr.2022.03.045

tion must be paid to residual stresses. They are of particular importance as they can strongly influence both static and fatigue strength of a component [26, 21], playing a key role in crack nucleation, modifying the crack orientation and propagation rate near the weld bead. Tensile residual stresses can lead to unexpected component failures when combined with in-service loading. In facts, they increase stresses at critical points in the material. In contrast, compressive residual stresses are sometimes sought after as they can provide benefits and improve the fatigue life [3, 27, 20, 25]. Experimental tests alone does not allow a complete evaluation of residual stresses within a component. However, in recent decades, the evaluation of residual stresses using numerical approaches has become widespread. Major examples include: casting problems [23, 16], welding [7, 6, 17, 1] and additive manufacturing [24, 29, 22]. Numerical analysis of residual stresses is made challenging by the multi-physics environment involved. Nevertheless, numerical methods have recently been employed much more often in the evaluation of residual stresses [13, 11] precisely due to the capabilities improvement of computers.

In this paper, a numerical and experimental analysis concerning the influence of residual stresses on the fatigue life assessment of S355JR structural steel components is presented. The aim was to determine under which loading conditions residual stresses had an influence on the fatigue life. The experimental fatigue assessment for the specific case of a welded tube-to-plate joint under as-welded and stress-relieved conditions, and for a notched specimen is discussed (both for a load ratio $R = -1$). Numerical analyses are presented and compared with experimental results for the case of welded joints. In particular, an uncoupled thermal-structural simulation was performed to evaluate the residual stresses due to the welding process. While in the case of the notched specimen a compressive preload was used to introduce a local residual stress field. In addition, this work represents a validation of the recently developed thermal-structural model studied by the same authors in [8, 11].

2. Material and model

The specimens considered for this work are shown in Figure 1 and consist of a welded tube-to-plate joint and a notched specimen, both made of S355JR structural steel. The welded specimen was produced by a partial penetration GMA-welding, connecting a tube together with a quadrangular plate. The dimensions of the tube are 44 mm of internal diameter and 10 mm of wall thickness. With regard to the plate, it has a side of 190 mm and a thickness of 25 mm. As shown in Figure 1b four holes have been drilled to allow the specimen to be clamped on the test bench of Figure 1a. In addition, a circular plate was placed at the top of the tube to allow the attachment between the actuators and the specimen, through a loading arm. The test bench is home-made, consisting of two independent hydraulic actuators which enable pure bending, pure torsion or a mix of these loads [14, 15, 5, 4].

The notched specimen has a maximum outer diameter of 22 mm and a notch diameter of 16 mm. The notch radius has a dimension of 0.2 mm and an opening angle of 35°. In this case the tests were carried out using a Shenk 250L/2T allowing to load the specimen in tension/compression and torsion.

The macroscopic failure surfaces of the two types of specimen are shown in Figure 2: figure 2a and Figure 2b show the fracture surfaces for a pure torsion load in both specimen geometries, while Figure 2c shows the fracture surface of the notched specimen for a tensile/compression load and Figure 2d that of the welded joint in the case of pure bending. A similarity between failure surfaces can be noticed. Figure 2a and Figure 2b show the factory-roof type of fracture with multiple cracks initiation and frequent plane transitions. Globally, cracks grow via mode III showing high interlocking, while they grow via mode I locally. On the contrary, Figure 2c and Figure 2d show few crack initiation points (i.e. in the most stressed area) and a global and local mode I for crack propagation, which contributes to a rapid crack growth.

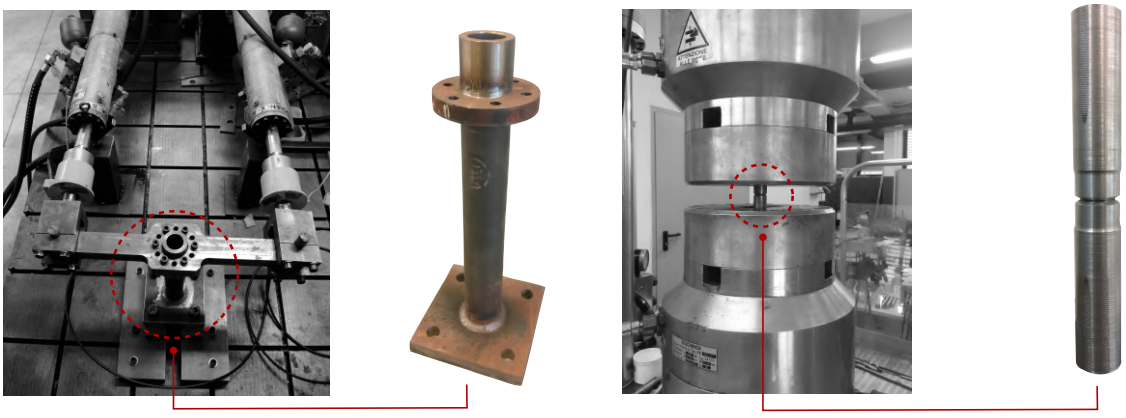

Fig. 1: Test-bench employed for fatigue testing of welded joints (a), pipe-to-plate welded joint (b), test-bench employed for fatigue testing of notched specimens (c), notched specimen (d)

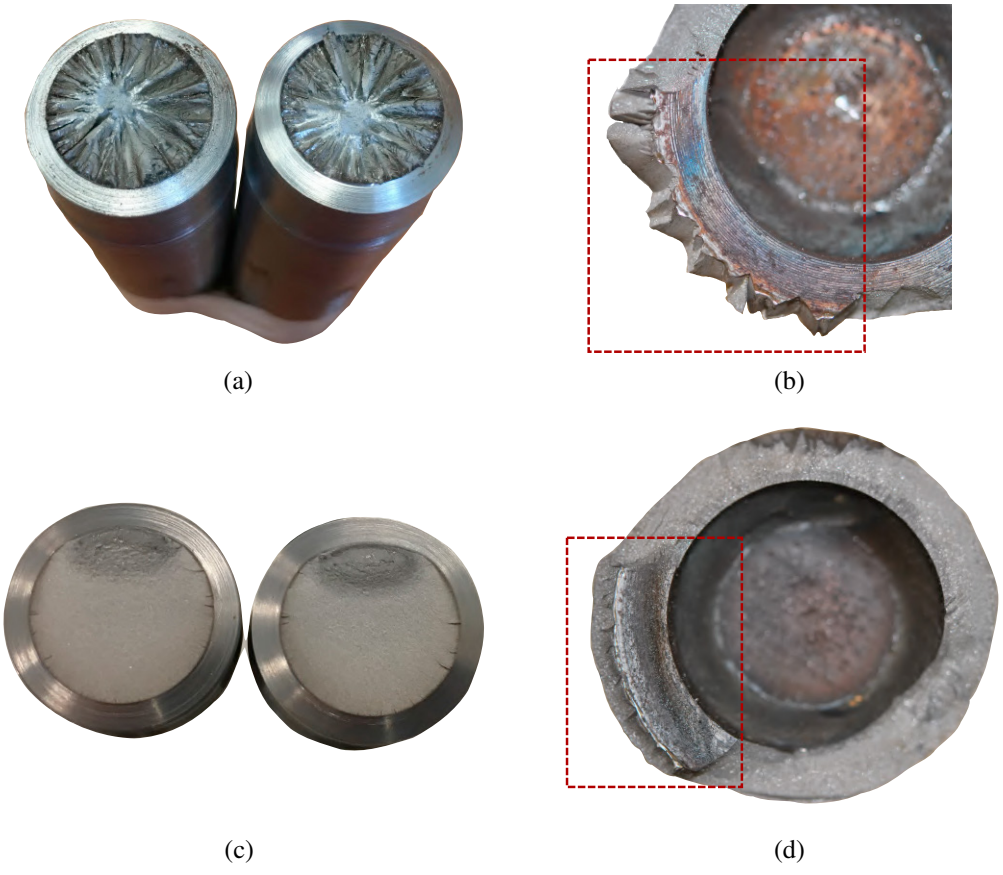

Fig. 2: Fracture surface for a torsion loaded notch specimen (a), fracture surface for a torsion loaded welded joint (b), fracture surface for a tensile/compressive loaded notch specimen (c), fracture surface for a bending loaded welded joint (d)

3. Finite element model

3.1. Thermal-structural analysis

A finite element model was developed to determine the residual stress field produced by the welding process. The numerical analysis (Figure 3) was based on a thermal-structural uncoupled simulation, in which the purely thermal model was solved as the first step, followed by the structural simulation. The model uses the ”element birth & death” technique to simulate the bead deposition process. As a final step a material removal analysis was used in order to validate the numerical model by comparing relaxed strain results between numerical and experimental analysis. In the following, the various aspects of the model will not be described in detail as they have been the subject of previous works [11, 8, 10, 9]. However, it is important to note that the thermal model used for this simulation does not employ classical heat sources such as Goldak or Gaussian; instead, it uses a simplified constant initial temperature (CIT) method, where elements have been activated at a fixed temperature T_i. The initial temperature is a fictitious temperature which incorporates all the simplifying assumptions of the model (i.e. simplified weld bead geometry, phase transitions, simplified material deposition process, uncertainties about material properties). The value of T_i has been obtained by best fitting experimental results of temperature calculated during the welding process. One can refer to [8] to observe that thermally, no substantial differences exist between the Goldak, Gaussian and CIT heat sources in a region far from the weld bead. From the developed thermal-structural model, the whole range of residual stresses was derived for the welded component, as shown in Figure 4. Specifically, the presented stresses are the radial and hoop ones, starting from the weld toe on the plate surface up to the plate end. It can be noted that maximum stresses were obtained in the weld notch, with both high stress values and gradients. These effects are mainly due to the process the material undergoes during melting and subsequent resolidification, and partly due to the perfectly sharp notch design in the finite element model. The latter was a necessary simplification required within the simulation designs step, which allowed the model to be solved within a reasonable calculation time. The introduction of a more correct notch geometry was performed in the subsequent step of the analysis described in section 3.2.

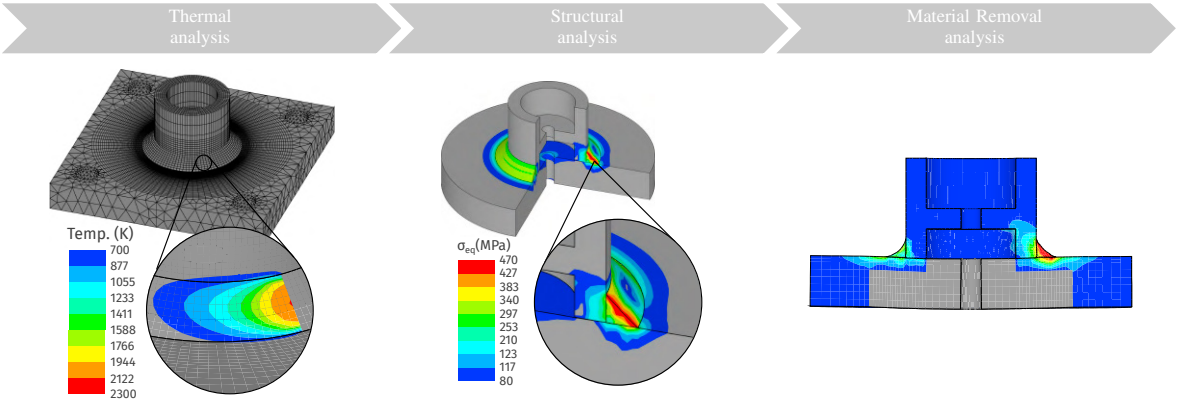

Fig. 3: Flowchart of the uncoupled thermal-structural simulation used for residual stresses evaluation

3.2. Fatigue analysis of the tube-to-plate welded joint

Following the thermal-structural analysis, a numerical investigation was carried out to determine critical plane damage factors. In order to simulate the specimen under as-welded conditions, the previously calculated residual stress data were mapped and then initialized within the numerical model intended for fatigue damage calculation. On the other hand, residual stress initialization step was omitted to simulate the stress-relieved conditions. As shown in Figure 5, the introduction of a sub-model was needed for the calculation of damage factors. In facts, a more realistic geometry of the weld bead was required in this case (i.e. fillet radii). The overall analysis consists of a linear-elastic model, in which the same mesh grid was imported from the structural analysis of section 3.1. Two remote force loads

(i.e. to simulate actuator loads) and four bolt constraints (i.e. to simulate the connection between specimen and test-bench) were introduced as boundary conditions. In the subsequent submodel analysis, only the most stressed volume during bending loading was modelled (i.e. while nominally there is no difference for torsion loading). Exploratory analyses were carried out to evaluate the critical notch in the various load and heat treatment configurations. The weld root was found to be the most critical region under all load and heat treatment combinations and it will be considered the reference region for the following analyses.

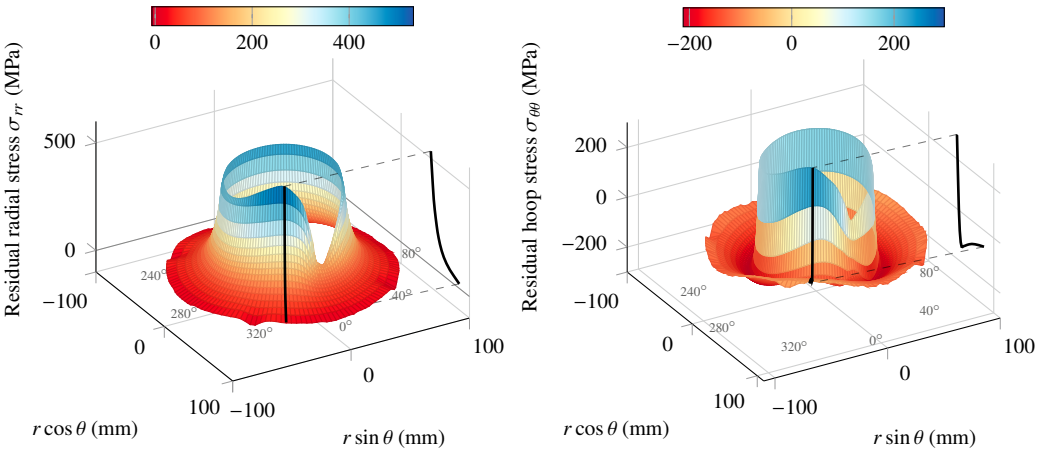

Fig. 4: Residual radial and hoop stresses on the plate surface starting from the weld toe, r and θ represent the radial and circumferential coordinates respectively

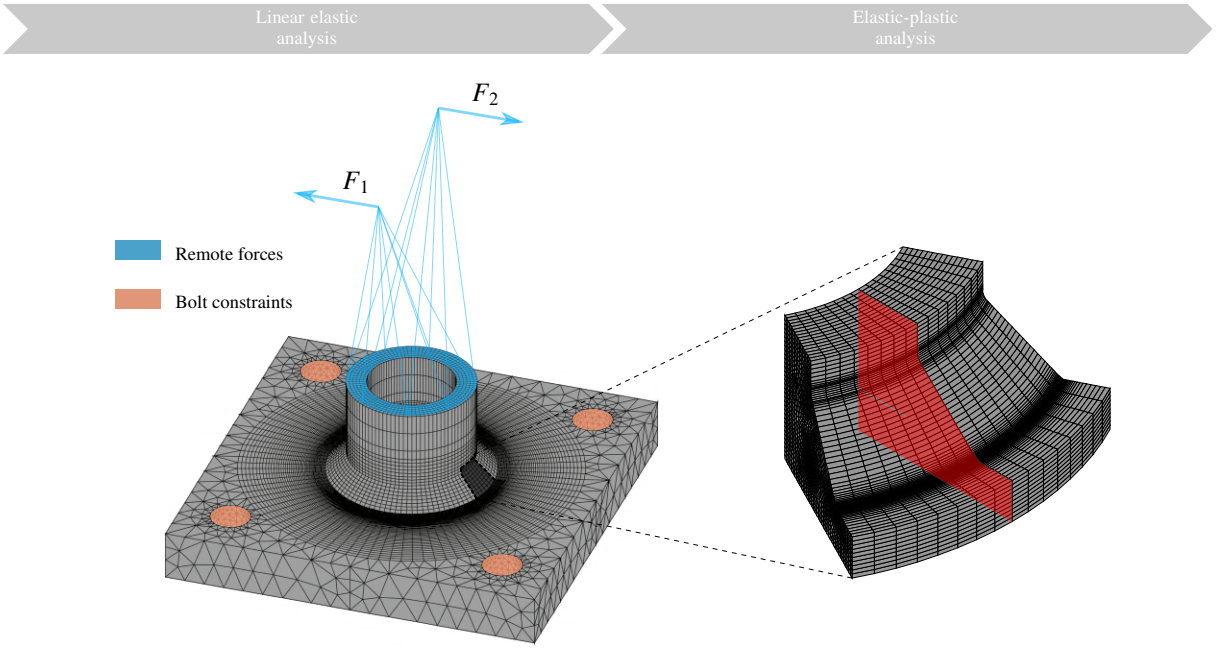

Fig. 5: Flowchart of the linear elastic and elastic-plastic models used to simulate the welded joint in as-welded and stress relieved conditions under fatigue loadings

3.3. Analysis of the notched specimen

In order to achieve comparable residual stress conditions to the welded joint, a notched specimen was designed (Figure 6). The size of the notch resembles that of the weld root, thus obtaining a similar-sized plastic region. To carry out an exploratory analysis on residual stress generation, a preload method was investigated. With this method a compressive preload was used to obtain tensile residual stresses in the vicinity of the notch. This loading mode was used together with torsion and traction/compression fatigue loading. Some preliminary results are presented below in section 4.1.
Numerical models were developed in order to evaluate the plastic area surrounding the notch. A 2D model (Figure 6b) was developed to investigate combined static and tensile/compression fatigue loading, while a 3D model (Figure 6a) was developed for the combined static and torsional fatigue loading. The numerical models used elastic-plastic material properties obtained from tensile tests carried out S355JR specimens. Both finite element models used quadratic elements, in particular the 3D model implemented 93240 elements and 389175 nodes, while the 2D model implemented 4090 elements and 12417 nodes.

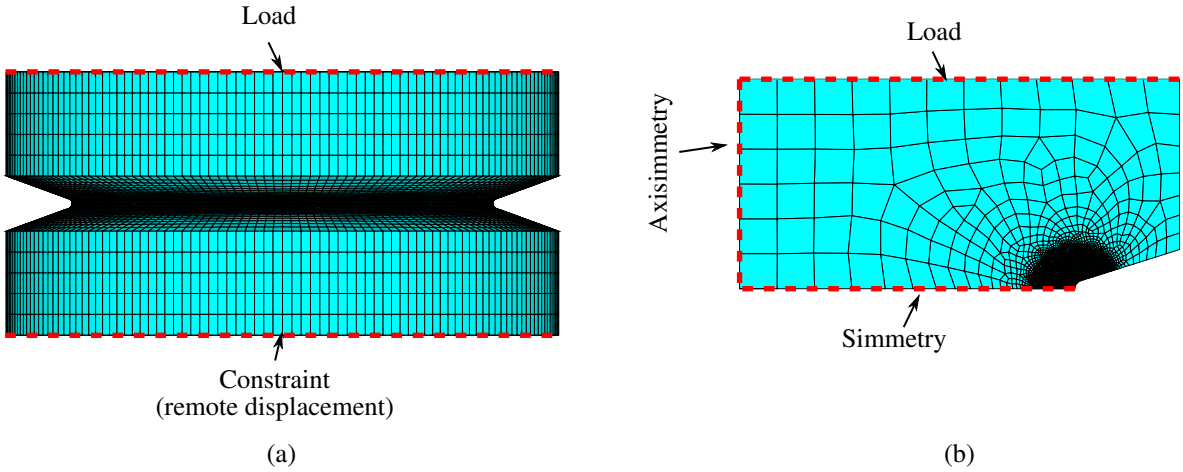

Fig. 6: 3D finite element model of the notched specimen used for simulating torsional loading (a), 2D finite element model of the notched specimen used for simulating traction/compression loading (b)

3.4. Tube-to-plate welded joint

With regard to welded joints, a different response between as-welded and stress-relieved specimens was obtained both experimentally (Figure 7) and numerically (Figure 8). Figure 7 shows nominal stresses over the number of cycles to break-trough for welded joints tested under pure torsion and pure bending in as-welded and stress-relieved conditions. It can be noticed that for the case of pure bending no difference is visible between as-welded and stress relieved conditions. On the other hand, for the pure torsion case, the stress relieved data were affected by an improvement in fatigue life. This can be clearly observed from the graph *Expected vs. Experimental number of cycles to break-trough*. Here stress relieved torsion data remains outside the scatter band generated by both bending and torsion as-welded results. Two scatter band lines can be observed, a dashed line was used to defined the scatter band of pure bending as-welded results while a continuous line to define the scatter band of pure torsion as-welded results.
Consistent results were obtained from a purely numerical analysis, examining Findley's critical plane factor for different load conditions. Figure 8 shows Findley's critical plane factor over the nominal stress range for pure bending and pure torsion loading in as-welded and stress relieved conditions. The maximum relative difference is also reported for the presented configurations. It is clearly visible how in the case of pure torsion the heat treatment provides a decrease in the damage factor at equal nominal stress range.

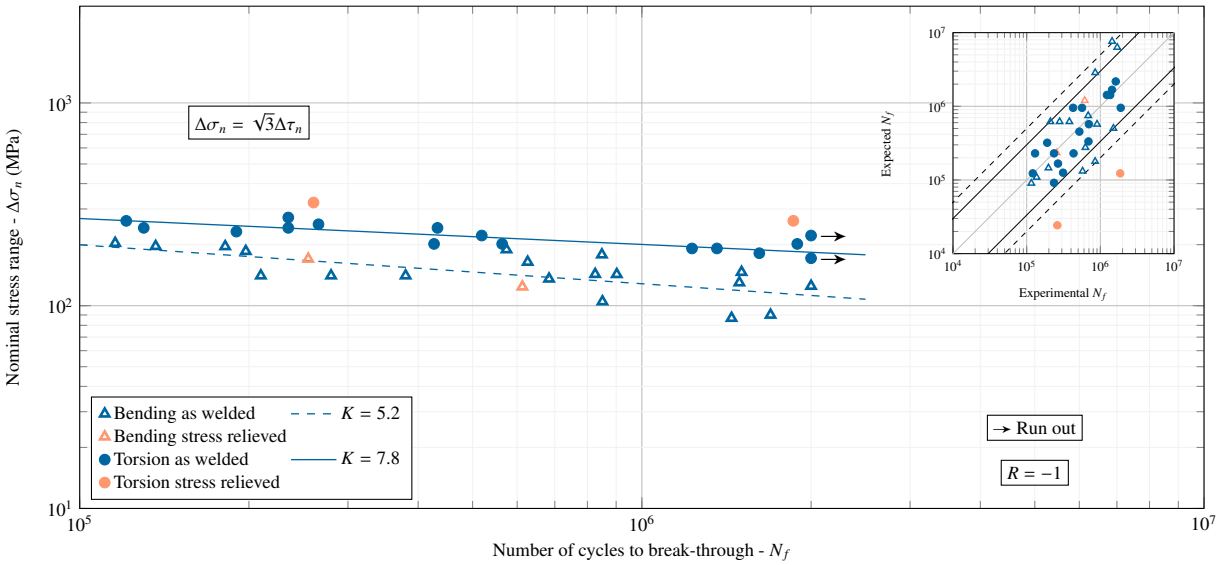

Fig. 7: Nominal stress range over number of cycles to break-through for pure bending and pure torsion fatigue loading in as-welded and stress relieved conditions

4. Results

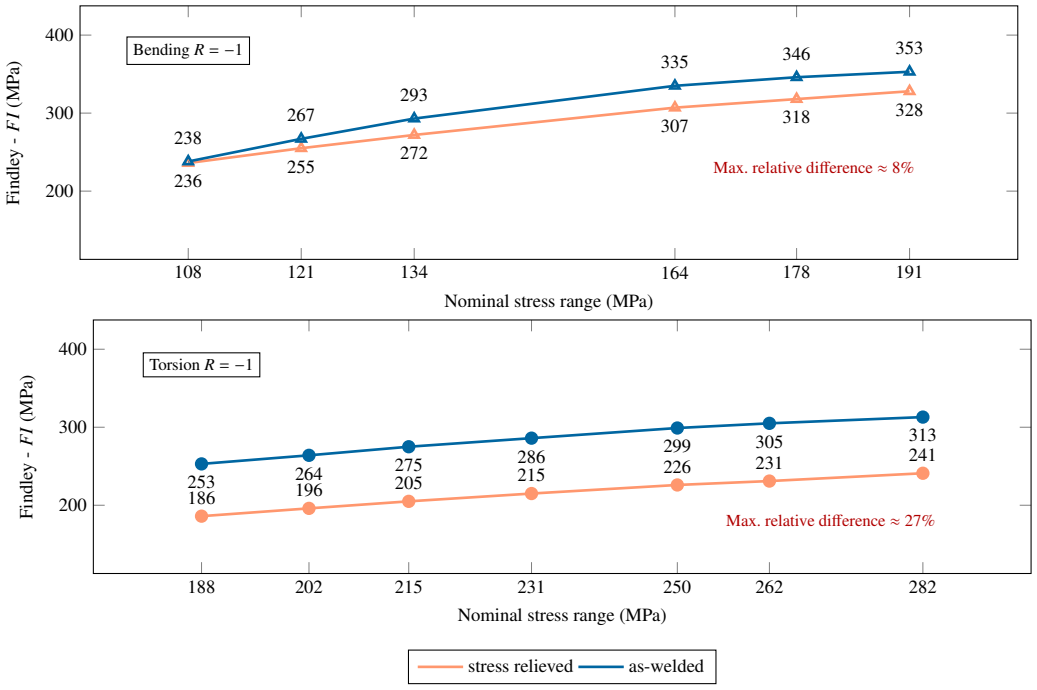

Fig. 8: Findley's critical plane factor over nominal stress range for pure bending and pure torsion loading in as-welded and stress relieved conditions

4.1. Notched specimen

In the following section, numerical results deriving from the finite element models presented in section 3.3 are provided. Figure 9 shows the hydrostatic stress variation over the radial coordinate in the notch area. Figure 9a represents the effect of a pure torsion load. It can be seen that under null preload, the hydrostatic stress is always close to zero (i.e. nominally zero). It should be noted that preload refers to a compressive loading followed by unloading, preceding the application of the fatigue load. If preloaded the specimen shows a pattern of hydrostatic stress. With a preloading of −35 MPa a maximum value of 177 MPa in hydrostatic stress is reached. However, these values are scarcely affected by the pure torsional load (i.e. as can be seen comparing blue and dashed red line of Figure 9a). It can therefore be assumed that, based on the stress triaxiality factor, the configuration with preload is more critical respect to the configuration without preload, if pure torsional loading is considered.
In contrast, with traction/compression loading, the hydrostatic stress field generated by the preload is affected by the fatigue loading. It should be noted that, the difference in hydrostatic stress considering the configurations with and without preload under fatigue loading is smaller if compared to the pure torsion configuration. This means that the load in this case affects the residual stress field produced by the preloading and that therefore the conditions with and without preload become similarly critical. Naturally, these considerations have been done by incorporating material plasticity within the numerical simulations and accounting for a sufficiently large number of fatigue cycles in order to stabilise the material.

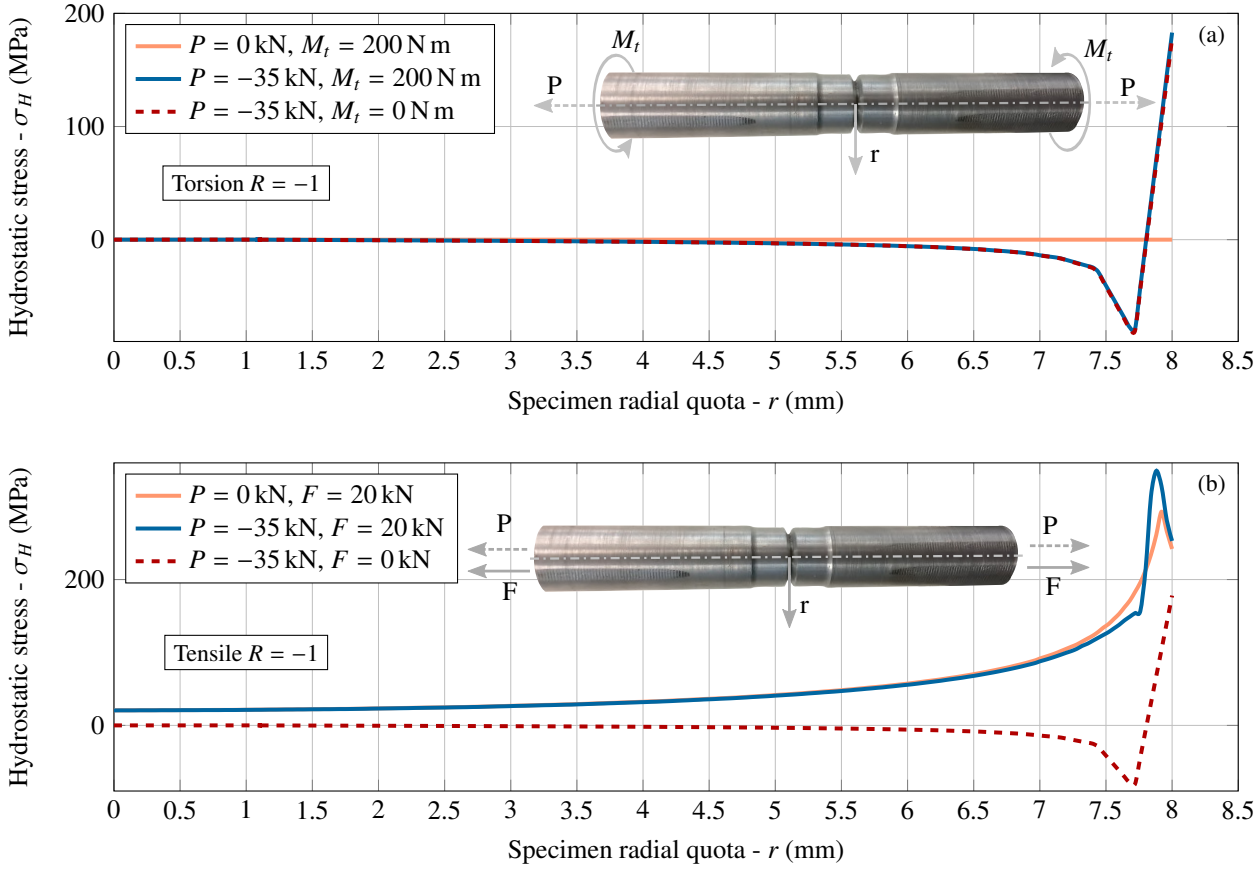

Fig. 9: Hydrostatic stress over notch radial coordinate for three different load configurations in pure torsion loading (a), hydrostatic stress over notch radial coordinate for three different load configurations in traction/compression loading

5. Conclusion

In this paper, results of the experimental and numerical influence of residual stresses on the fatigue life of welded joints and notched specimens were reported. In order to better understand the outcomes obtained from the welded joints, an exploratory study was carried out on a simpler notched specimen geometry, in presence of a compressive preload. From the analysis conducted it can be concluded that:

- the thermal-structural model implemented, although simplified, allows the simulation of the welding process and thus enables to understand the numerical effect of residual stresses on the fatigue life of the welded joint;
- residual stresses showed a larger effect on fatigue life if a pure torsion load is considered rather than a pure bending load;
- if stress triaxiality is considered as a fatigue damage factor, a higher difference between as-welded and stress relieved specimen is found by implementing pure torsion loading; in facts, torsion load alone is not able to alter the hydrostatic stress field produced by the initial residual stresses.

References

[1] Ansaripour, N., Heidari, A., Eftekhari, S.A., 2020. Multi-objective optimization of residual stresses and distortion in submerged arc welding process using Genetic Algorithm and Harmony Search. Proceedings of the Institution of Mechanical Engineers, Part C: Journal of Mechanical Engineering Science 234, 862–871. doi:10.1177/0954406219885977.

[2] Barsoum, Z., Barsoum, I., 2009. Residual stress effects on fatigue life of welded structures using LEFM. Engineering Failure Analysis 16, 449–467. doi:10.1016/j.engfailanal.2008.06.017.

[3] Bartolozzi, R., Frendo, F., 2011. Stiffness and strength aspects in the design of automotive coil springs for McPherson front suspensions: A case study. Proceedings of the Institution of Mechanical Engineers, Part D: Journal of Automobile Engineering 225, 1377–1391. doi:10.1177/0954407011403853.

[4] Bertini, L., Cera, A., Frendo, F., 2014. Experimental investigation of the fatigue resistance of pipe-to-plate welded connections under bending, torsion and mixed mode loading. International Journal of Fatigue 68, 178–185. doi:10.1016/j.ijfatigue.2014.05.005.

[5] Bertini, L., Frendo, F., Marulo, G., 2016. Effects of plate stiffness on the fatigue resistance and failure location of pipe-to-plate welded joints under bending. International Journal of Fatigue 90, 78–86. doi:10.1016/j.ijfatigue.2016.04.015.

[6] Bhatti, A.A., Barsoum, Z., Murakawa, H., Barsoum, I., 2015. Influence of thermo-mechanical material properties of different steel grades on welding residual stresses and angular distortion. Materials and Design 65, 878–889. doi:10.1016/j.matdes.2014.10.019.

[7] Capriccioli, A., Frosi, P., 2009. Multipurpose ANSYS FE procedure for welding processes simulation. Fusion Engineering and Design 84, 546–553. doi:10.1016/j.fusengdes.2009.01.039.

[8] Chiocca, A., Frendo, F., Bertini, L., 2019a. Evaluation of heat sources for the simulation of the temperature distribution in gas metal arc welded joints. Metals 9, 1142. doi:10.3390/met9111142.

[9] Chiocca, A., Frendo, F., Bertini, L., 2019b. Evaluation of residual stresses in a tube-to-plate welded joint. MATEC Web of Conferences 300, 19005. doi:10.1051/matecconf/201930019005.

[10] Chiocca, A., Frendo, F., Bertini, L., 2020. Experimental evaluation of relaxed strains in a pipe-to-plate welded joint by means of incremental cutting process. Procedia Structural Integrity 28, 2157–2167. doi:10.1016/j.prostr.2020.11.043.

[11] Chiocca, A., Frendo, F., Bertini, L., 2021. Evaluation of residual stresses in a pipe-to-plate welded joint by means of uncoupled thermal-structural simulation and experimental tests. International Journal of Mechanical Sciences 199, 106401. doi:10.1016/j.ijmecsci.2021.106401.

[12] Chlup, Z., Novotná, L., Šiška, F., Drdlík, D., Hadraba, H., 2020. Effect of residual stresses to the crack path in alumina/zirconia laminates. Journal of the European Ceramic Society 40, 5810–5818. doi:10.1016/j.jeurceramsoc.2020.06.044.

[13] Ferro, P., Berto, F., 2016. Quantification of the Influence of Residual Stresses on Fatigue Strength of Al-Alloy Welded Joints by Means of the Local Strain Energy Density Approach. Strength of Materials 48, 426–436. doi:10.1007/s11223-016-9781-0.

[14] Frendo, F., Bertini, L., 2015. Fatigue resistance of pipe-to-plate welded joint under in-phase and out-of-phase combined bending and torsion. International Journal of Fatigue 79, 46–53. doi:10.1016/j.ijfatigue.2015.04.020.

[15] Frendo, F., Marulo, G., Chiocca, A., Bertini, L., 2020. Fatigue life assessment of welded joints under sequences of bending and torsion loading blocks of different lengths. Fatigue and Fracture of Engineering Materials and Structures 43, 1290–1304. doi:10.1111/ffe.13223.

[16] Greß, T., Glück Nardi, V., Schmid, S., Hoyer, J., Rizaiev, Y., Boll, T., Seils, S., Tonn, B., Volk, W., 2021. Vertical continuous compound casting of copper aluminum bilayer rods. Journal of Materials Processing Technology 288, 116854. doi:10.1016/j.jmatprotec.2020.116854.

[17] Hemmesi, K., Mallet, P., Farajian, M., 2020. Numerical evaluation of surface welding residual stress behavior under multiaxial mechanical loading and experimental validations. International Journal of Mechanical Sciences 168, 105127. doi:10.1016/j.ijmecsci.2019.105127.

[18] Le, T., Paradowska, A., Bradford, M.A., Liu, X., Valipour, H.R., 2020. Residual stresses in welded high-strength steel I-Beams. Journal of Constructional Steel Research 167, 105849. doi:10.1016/j.jcsr.2019.105849.

[19] Lillemäe, I., Lammi, H., Molter, L., Remes, H., 2012. Fatigue strength of welded butt joints in thin and slender specimens. International Journal of Fatigue 44, 98–106. doi:10.1016/j.ijfatigue.2012.05.009.

[20] Liu, D., Liu, D., Guagliano, M., Xu, X., Fan, K., Bagherifard, S., 2021. Contribution of ultrasonic surface rolling process to the fatigue properties of TB8 alloy with body-centered cubic structure. Journal of Materials Science and Technology 61, 63–74. doi:10.1016/j.jmst.2020.05.047.

[21] Lopez-Jauregi, A., Esnaola, J.A., Ulacia, I., Urrutibeascoa, I., Madariaga, A., 2015. Fatigue analysis of multipass welded joints considering residual stresses. International Journal of Fatigue 79, 75–85. doi:10.1016/j.ijfatigue.2015.04.013.

[22] Razavi, S.M., Van Hooreweder, B., Berto, F., 2020. Effect of build thickness and geometry on quasi-static and fatigue behavior of Ti-6Al-4V produced by Electron Beam Melting. Additive Manufacturing 36, 101426. doi:10.1016/j.addma.2020.101426.

[23] Ridgeway, C.D., Gu, C., Ripplinger, K., Detwiler, D., Ji, M., Soghrati, S., Luo, A.A., 2020. Prediction of location specific mechanical properties of aluminum casting using a new CA-FEA (cellular automaton-finite element analysis) approach. Materials and Design 194, 108929. doi:10.1016/j.matdes.2020.108929.

[24] Schnabel, K., Baumgartner, J., Möller, B., 2019. Fatigue Assessment of Additively Manufactured Metallic Structures Using Local Approaches Based on Finite-Element Simulations, in: Procedia Structural Integrity, Elsevier B.V.. pp. 442–451. doi:10.1016/j.prostr.2019.12.048.

[25] Song, M., Wu, L., Liu, J., Hu, Y., 2021. Effects of laser cladding on crack resistance improvement for aluminum alloy used in aircraft skin. Optics and Laser Technology 133, 106531. doi:10.1016/j.optlastec.2020.106531.

[26] Sonsino, C.M., 2009. Effect of residual stresses on the fatigue behaviour of welded joints depending on loading conditions and weld geometry. International Journal of Fatigue 31, 88–101. doi:10.1016/j.ijfatigue.2008.02.015.

[27] Soyama, H., Chighizola, C.R., Hill, M.R., 2021. Effect of compressive residual stress introduced by cavitation peening and shot peening on the improvement of fatigue strength of stainless steel. Journal of Materials Processing Technology 288, 116877. doi:10.1016/j.jmatprotec.2020.116877.

[28] Vila Real, P.M., Cazeli, R., Simoes da Silva, L., Santiago, A., Piloto, P., 2004. The effect of residual stresses in the lateral-torsional buckling of steel I-beams at elevated temperature. Journal of Constructional Steel Research 60, 783–793. doi:10.1016/S0143-974X(03)00143-3.

[29] Wagener, R., Hell, M., Scurria, M., Bein, T., 2020. Deriving the Structural Fatigue Behavior of Additively Manufactured Components, in: Minerals, Metals and Materials Series, Springer. pp. 139–149. doi:10.1007/978-3-030-36296-6_13.